



HAL
open science

Hybridization of additive manufacturing processes to build ceramic/metal parts: Example of LTCC

Jonathan Raynaud, Vincent Pateloup, Mégane Bernard, Delphine Gourdonnaud, Damien Passerieux, Dominique Cros, Valérie Madrangeas, Thierry Chartier

► To cite this version:

Jonathan Raynaud, Vincent Pateloup, Mégane Bernard, Delphine Gourdonnaud, Damien Passerieux, et al.. Hybridization of additive manufacturing processes to build ceramic/metal parts: Example of LTCC. Journal of the European Ceramic Society, 2020, 40 (3), pp.759-767. 10.1016/j.jeurceramsoc.2019.10.019 . hal-02432445

HAL Id: hal-02432445

<https://hal.science/hal-02432445>

Submitted on 9 Dec 2020

HAL is a multi-disciplinary open access archive for the deposit and dissemination of scientific research documents, whether they are published or not. The documents may come from teaching and research institutions in France or abroad, or from public or private research centers.

L'archive ouverte pluridisciplinaire **HAL**, est destinée au dépôt et à la diffusion de documents scientifiques de niveau recherche, publiés ou non, émanant des établissements d'enseignement et de recherche français ou étrangers, des laboratoires publics ou privés.

Hybridization of additive manufacturing processes to build ceramic/metal parts: Example of LTCC

Jonathan Raynaud¹, Vincent Pateloup¹, Mégane Bernard¹, Delphine Gourdonnaud¹, Damien Passerieux², Dominique Cros², Valérie Madrangeas², Thierry Chartier¹,

¹ CNRS, University of Limoges, Institute of Research for Ceramics (IRCER), UMR 7315, European Ceramics Center, Limoges, France

² CNRS, University of Limoges, XLim, UMR 7252, Limoges, France

Abstract

Stereolithography is an additive manufacturing process, which makes it possible to fabricate useful complex 3D ceramic parts with a high dimensional resolution and a good surface finish. By coupling the latter process with a second, to deposit another material, it will be possible to obtain multi-material parts using a hybrid machine. This machine is therefore composed of two additive manufacturing processes: stereolithography and robocasting. During this work, we decided to study ceramic - metal assemblies and more particularly the LTCC materials. These materials have low sintering temperatures, generally less than 1000 °C. The mechanical and electrical properties will be studied of the development of parts with complex and innovative geometries to improve the characteristics of current circuits. Finally, our substrate have an excellent permittivity ($\epsilon_r=5.05$) and dielectric loss ($\tan \delta=1.8 \cdot 10^{-3}$).

1. Introduction

The "Temperature Cofired Ceramic" multilayer technologies appeared around the beginning of the 90s. These processes consist in stacking ceramic dielectric sheets elaborated by tape casting, on which conductive patterns, resistances or capacities, were printed by screen-printing (Figure 1). The different printed tapes are assembled and laminated to obtain multilayers circuits. Then metallized holes through the layers, called vias, allow connections between different conductive patterns in different dielectric layers. After lamination, the green stack is submitted to a heat treatment in a controlled atmosphere to eliminate organic and densify components. Co-sintering can be carried out at high temperature ($T > 1000$ °C) for High Temperature Cofired Ceramics (HTCC) or at low temperature ($T \leq 1000$ °C) for Low Temperature Cofired Ceramics (LTCC). The choice of sintering temperature depends on the temperature of use of the component. HTCC parts are used in the power assembly for aerospace [1]. The LTCC technology is widely used in the manufacture of high frequency devices such as Bluetooth antenna modules, transmitters, power amplifiers, filters and other applications [1,2,3]. The dielectric and conductive materials are different for LTCC

(alumina/glass and silver, copper or gold) and HTCC (alumina and tungsten or molybdenum), components depending on the temperature of sintering.

The classical route to manufacture HTCC and LTCC parts, i.e. tape casting process for the ceramic substrate and screen-printing for the metallic tracks and vias [4] limits some characteristics of the components:

- 1) The thickness of a ceramic layer must be larger than 150 microns in order to properly manipulate the tape cast green sheet,
- 2) The shape of the metallic conductive pattern is limited to 2D patterns linked by vertical vias between dielectric layers which limit the complexity of the metallic network and then the electrical functions than can be integrated inside the LTCC component [1],
- 3) There is no possibility of developing lateral shielding,
- 4) It is impossible to get slanted vias.

In the context of manufacturing of LTCC or HTCC components, additive manufacturing makes it possible to automate production, to build more complex 3D metal circuits than the classical route, to build more complex ceramic packaging shapes and to decrease the thickness of each layer in comparison to classical route. Indeed, additive manufacturing processes gives access to specific architectures to improve properties or to introduce new functions with the deposition of the desired material at each voxel of the part during its construction. In addition, additive manufacturing allows the reduction of production costs because it does not require tooling and limits the loss of raw material.

The present work proposes the development of a new process based on the hybridization of two additive manufacturing processes, i.e. stereolithography and robocasting, to deposit 3D structures of ceramic and metallic materials. In order to evaluate the proposed hybrid process, the feasibility of multimaterial components by hybridization of the stereolithography and robocasting processes is focused on the elaboration of LTCC parts in the article. There is a growing interest to use additive manufacturing processes for LTCC material in many fields of applications (aeronautic, automotive, energy) [5]. For example, the works of R. Faddoul and al. have shown that it is possible to obtain silver tracks using flexography and inkjet printing [6–8] in order to reduce the sintering temperature and increase their conductivity with the use of nanoparticles because of their great reactivity.

This new hybrid process will be able to decrease the thickness of a ceramic layer down to 50 microns according to the metallic track thickness and to deposit metallic tracks with a thickness of 30–40 microns. The tracks will be connected by metallic vias with the same metal. It will also be possible to make all-metal layers. In order to show the possibilities offered by this new hybrid process associating stereolithography and robocasting, a hybrid machine has been

designed. Several test parts have been realized and characterized in terms of mechanical and electrical behavior to validate this one.

A demonstrative part composed of dielectric ceramic and conductive metal pattern is considered in order to evaluate the possibilities of the developed process (Figure 2).

This part is composed of a dielectric substrate (light blue), horizontal tracks (dark blue), oblique and vertical vias (red) and armored vias (black). However, for some preliminary tests, this complex geometry is decomposed in several stages with different difficulties.

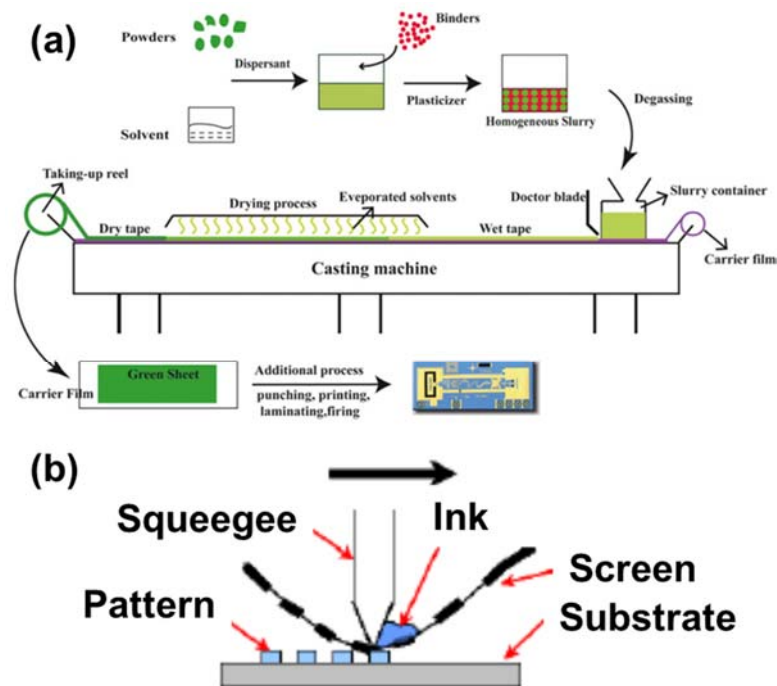


Figure 1: (a) Production cycle of an LTCC circuit board [4,9,10] and (b) Process of screen printing

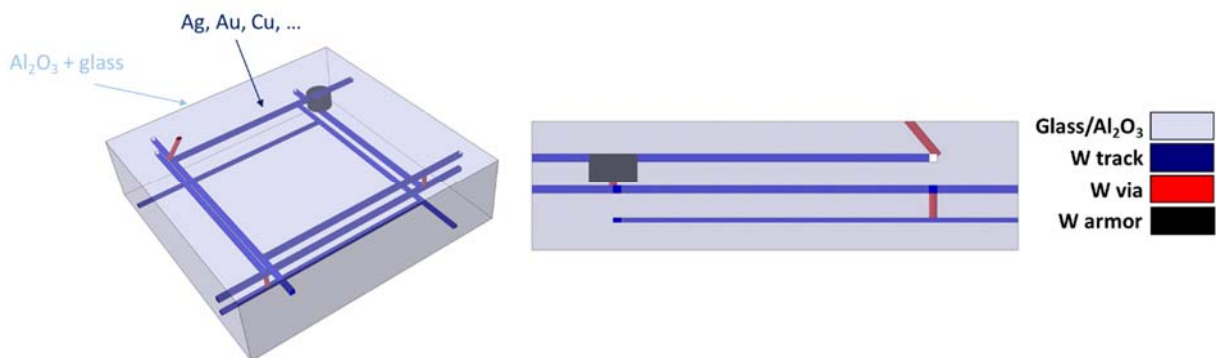


Figure 2: Design of the LTCC test component with a perspective view (a) and a section (b)

2. Materials and methods

2.1. Presentation of the hybrid machine

The two selected processes to manufacture glass/alumina and silver LTCC components are stereolithography and micro-extrusion. Before presenting the hybrid machine, a quick description of the two processes is carried out.

The stereolithography process is based on the selective polymerization, by a computer controlled UV light, of a curable suspension [11-13]. Starting from the CAD file of the part to be realized, the green part is built layer upon layer with the polymerization of cross sectional patterns in each layer (Figure 3a). After completion of the part, the last stages correspond to the cleaning (removal of sticky non polymerized suspension), debinding and sintering. The stereolithography machine used has a laser UV source light, with a wavelength of 355 nm.

Robocasting consists in the extrusion of filaments through a nozzle having a diameter between 100 microns and few millimeters mounted on an X-Y-Z system. The first numerical stages (i.e. CAD, Stl,...) are identical to those using in stereolithography. A robocasting head has been specifically designed at laboratory to print the conductive metal patterns. This head allows the use of Techcon nozzles with a diameter between 0.1 and 1.5 mm. The schematics of the two processes employed are presented in Figure 3.

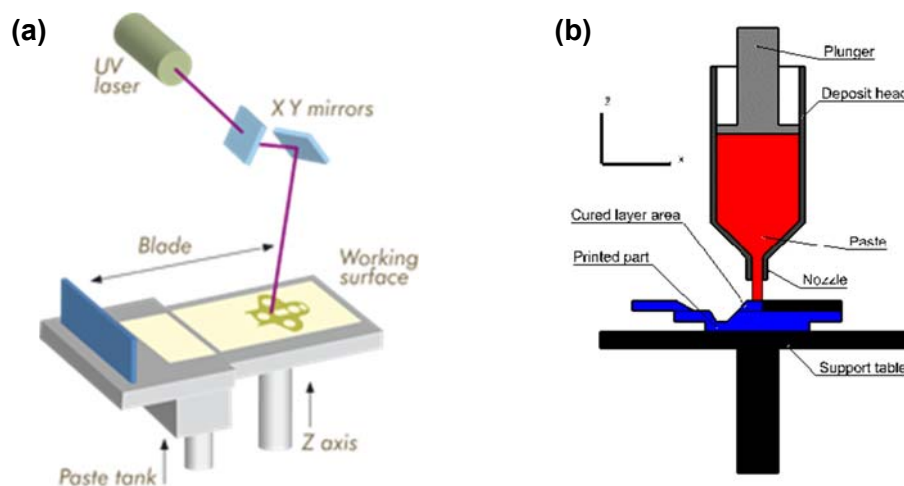


Figure 3: Principle of the processes of (a) stereolithography [14] and (b) robocasting

The hybridization of the two processes consists in a robotic arm controlling the micro extrusion head positioning coupled to a stereolithography device, as shown in Figure 4.

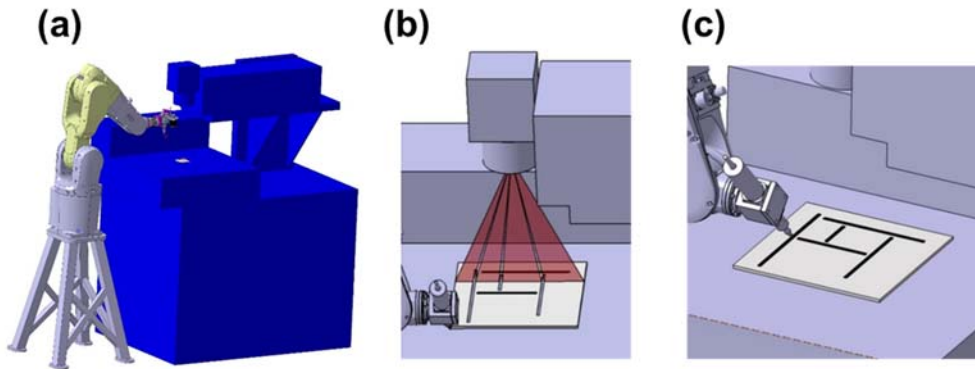


Figure 4 : Assembly for the production of bi-material objects combining robocasting and stereolithography processes

This assembly represented Figure 4.a contains on the right the stereolithography equipment for printing the ceramic layers (Figure 4.b) and, on the left, the robotic arm carrying the robocasting head making to deposit the metallic patterns (Figure 4.c).

The metallic network is defined as lines and vias in each layer. Lines and vias in which the metallic paste has to be deposited are not polymerized, then cleaned to remove the non-polymerized ceramic paste. After, the robot equipped with the extrusion head deposit a filament of metallic paste in the cleaned lines and vias. The strategy chosen to manufacture the complex part presented in Figure 2 is to decompose the manufacturing of this part in different steps of graduated complexity of the printed shapes (Figure 5). The final target is to build in one-step the part given in Figure 2.

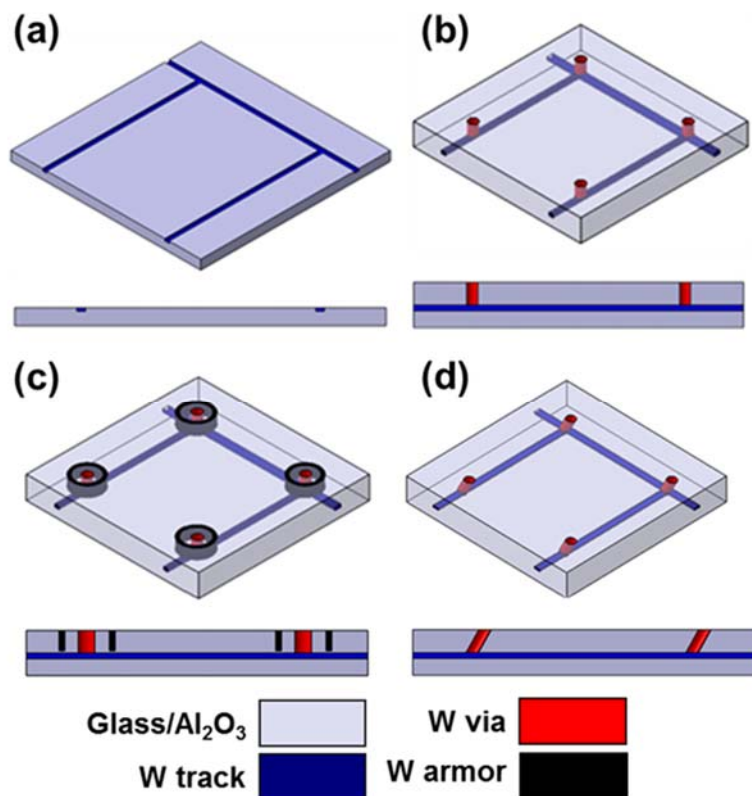


Figure 5: Presentation of different geometries studied: (a) Uncovered tracks, (b) Embedded tracks connected to the surface by vias, (c) Armored vias and (d) oblique vias. The metal is represented in dark blue, the substrate in light grey, vias in red and armor in black.

The first step consist in the deposition of an uncovered silver line on a glass/alumina substrate (Figure 5.a). The motif is defined in order to measure the conductivity of the track by the 4-points method and to observe its morphology. The second step proposes to embed the track between two alumina layers in order to evaluate the co-sintering between silver and glass/alumina and connect these tracks to the surface by vias (Figure 5.b). This geometry aims to validate the feasibility of vias and their connection with the track. The conductivity of the metallic circuit will be measured after sintering. The next two geometries cannot be obtained using by conventional methods and correspond to a significant improvement in the performance of current circuits. The third geometry correspond to continuous armored vias (Figure 5.c). The last geometry (Figure 5.d) is to realize oblique vias, which allow connecting two tracks with an x and y, shift.

A final geometry will allow the characterization of our materials in hyper-frequency (Figure 6). This part has been designed by XLim laboratory (Limoges; France) in order to produce optimal performances; these ones having been qualified by retro-simulation in high frequencies with the theoretical perfect geometry.

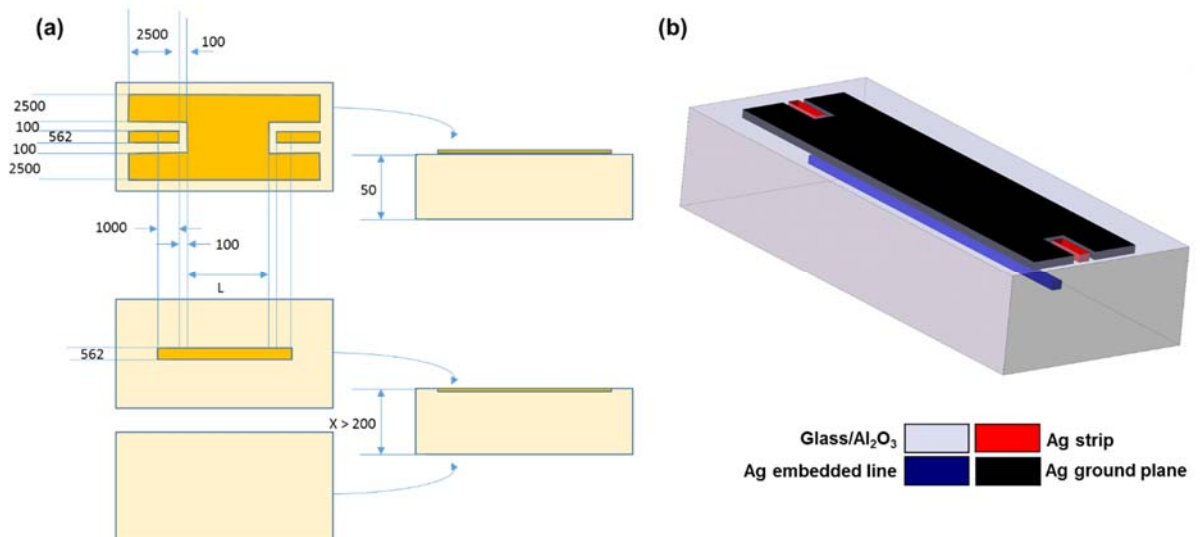


Figure 6 : Original geometries for hyper frequency characterization: embedded microstrip resonator with the dimensions given in micrometer range.

This geometry consists of a surface ground plane (in black) with, on both sides, coplanar access for measurement by microwave probes. The line, embedded in the dielectric substrate, is a half-wave resonator coupled to the coplanar access by evanescent modes. The analysis of the resonances (frequencies and quality factors) will make it possible to characterize the structure. This geometry can be obtained using the hybrid process and then characterized in the microwave range. Our goal is to obtain parts whose dimensions are as close as possible to those designed by the simulation. The choice of materials to reach the expected properties in the microwave is essential.

2.2. Ceramic paste for dielectric substrate

LTCC material conventionally used for the dielectric substrate is alumina mixed with a glassy phase [15]. The glasses generally used are borosilicate. Alumina may be added to improve mechanical properties [5]. Other glasses are also used and composed of heavier oxides such as Zn, Pb or Bi oxides [16]. The conductive tracks can be realized with metallic materials having a high electrical conductivity such as gold, silver, copper or a silver/palladium mixture [9].

The characteristics of the LTCC substrate material must be adapted to applications at high frequency:

- a low dielectric constant (ϵ_r) between 5 and 20 [17],
- a low dielectric loss ($\tan \delta$) between 10^{-3} – 10^{-4} and a dielectric constant temperature coefficient ($\tau\epsilon$) close to 0 [17,18].

Besides, the light absorption of this material in the UV range has to be low in order to make it possible the polymerization of the ceramic suspension during the stereolithography process [11]. Finally, it must have a sintering temperature below 1000 ° C [9], temperature that represents the melting point of the classical materials use at this temperature (silver, gold copper...). A first approach has been to evaluate, in terms of UV light absorption, a commercial LTCC powder (51K65, Heraeus, German) (Figure 7.a). The spectrometer used for this analysis is the model Cary 5000 UV-vis-IR, Agilent, USA.

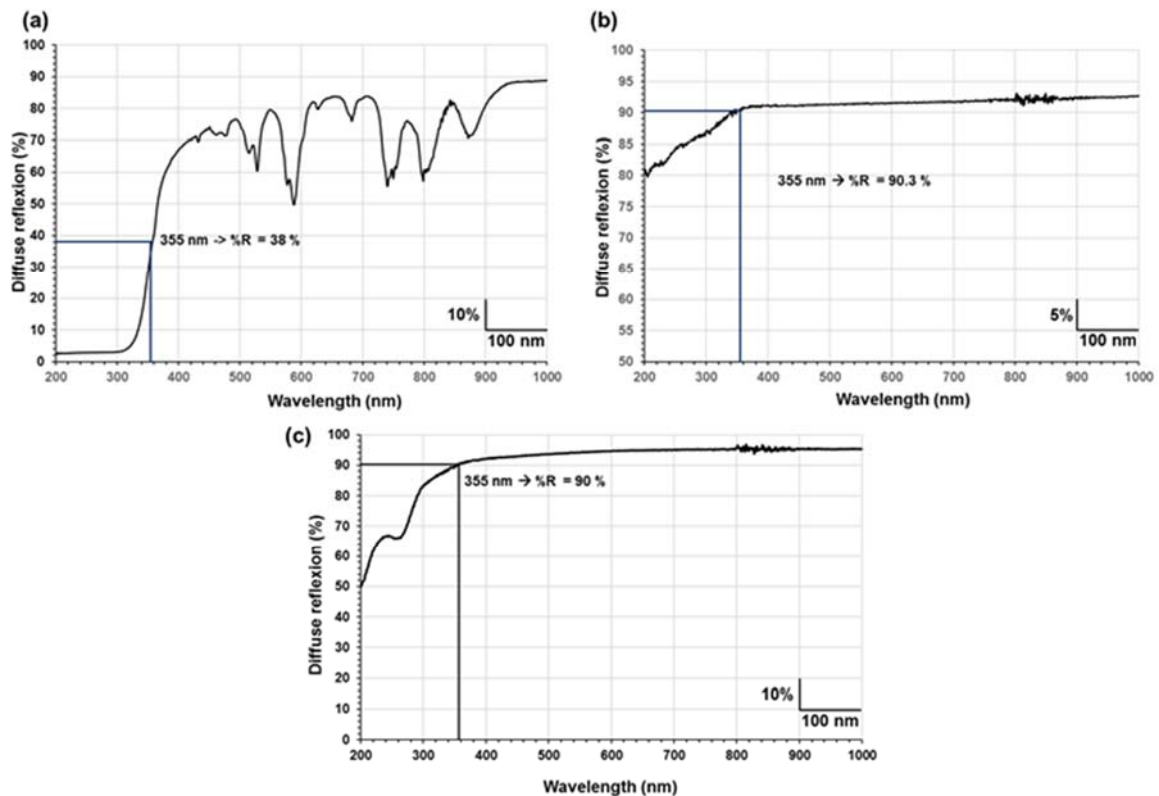


Figure 7: Spectrometry curve obtained by diffuse reflection on a) commercial Heraeus LTCC powder and b) borosilicate glass powder and c) alumina powder

The high absorption of this LTCC material at the wavelength of 355nm used by the stereolithography machine (%R = 38% and %Abs = 62 %) makes this material incompatible with the stereolithography process since more than 60% of the beam exposure density is absorbed at 355nm (Figure 7.a). An X-ray fluorescence analysis has confirmed the presence of many heavy elements that would absorb the light in the UV wavelength.

Then a formulation of LTCC material was developed, consisting in a mixture of alumina and a commercial glass, compatible with our stereolithography process. A fine reactive α -alumina powder was used (P152SB Alteo, France, $d_{50}=1.4\mu\text{m}$, Specific Surface Area BET = $2.60\text{ m}^2/\text{g}$, purity = 99.80%). A commercial borosilicate glass ($d_{50}=1.6\mu\text{m}$, Specific Surface Area BET = $8.75\text{ m}^2/\text{g}$) containing only light elements was added in order to avoid UV absorption by the glass. The absorption of alumina and glass at 355 nm (%R = 90% and %Abs = 10%) is very low (Figure 7.b and c) and adapted to the stereolithography process. The softening point of this glass is 920 °C. The co-sintering temperature will then be lower than 920°C.

In the literature, different proportions of glass mixed with alumina, ranging from 60 to 80% by mass, are proposed [2,3,9]. This amount will be selected depending on the desired shrinkage

during heat treatment. Now, the selection of the metal composing our tracks and vias can be treated.

2.3. Metallic paste for tracks and vias

The metallic tracks allow conduction of the current in the dielectric substrate. The glass was chosen to make it possible a densification of the dielectric alumina/glass mixture at a temperature of 850°C, which is compatible with silver as conductive metal. According to the process, the particle size of the silver powder and the formulation of the paste must allow extrusion through a 100 µm nozzle. The target track width and vias diameter are 100 µm after sintering.

In this respect, a commercial silver paste (ElectroScience, USA - ref. 9912-K) is tested. The paste contains 81.1 wt% silver and 18.9 wt% organic phase. The sintering temperature recommended by the provider is 850 °C for 1 hour. The selected material of substrate should therefore have a similar sintering temperature than the silver metal. The SEM micrograph (JEOL JSM-IT-300-LV) of the silver powder before heat treatment shows a mean silver particle size lower than 1µm (Figure 8), that is compatible with an extrusion of the paste through a 100 µm diameter nozzle.

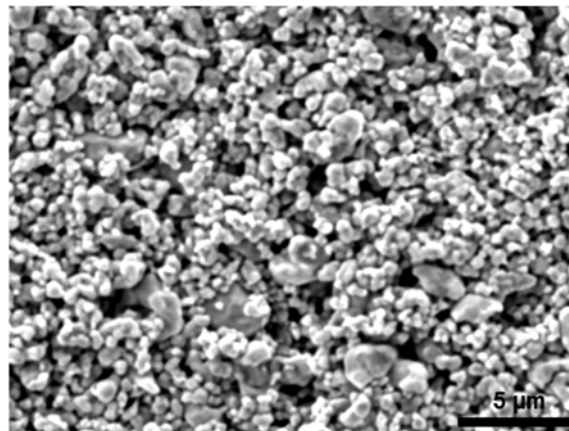


Figure 8: SEM Micrograph of the silver powder

3. Results

3.1. Printed parts

The substrates are printed by stereolithography with a layer thickness of 50 microns. The tracks are obtained by robocasting with a printed speed of 10 mm.s⁻¹ and a diameter nozzle of 100 µm. An observation of the tracks before thermal treatment are carried out by optical microscopy (Figure 9).

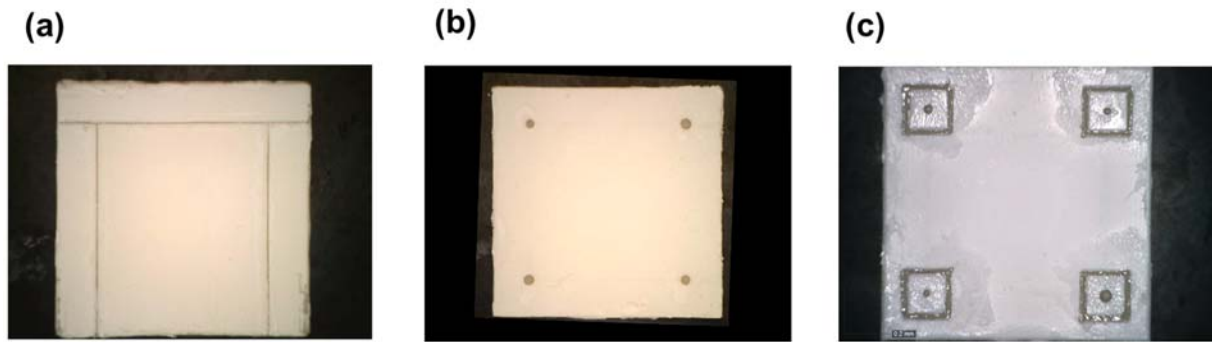


Figure 9: Micrograph of green parts (a) uncovered tracks, (b) Embedded tracks with vias and (c) Armored vias

The green tracks have a width of 150 microns (Figure 9.a) and vias with a diameter of 300 microns (Figure 9.b). Square armors have sides of 5 mm and a width of 300 microns (Figure 9.c). It then is necessary to determine the ideal thermal cycle for debinding and co-sintering of printed parts.

3.2. Thermal cycle – Debinding and sintering atmosphere

The first step was to determine the alumina/glass ratio of the substrate material in order to formulate the stereolithography paste. The substrate should have maximum densification after a heat treatment at 850 °C for one hour in air to be in line with the recommendations of the supplier of the metal paste. In this respect, dilatometric analysis (TMA1750, Setaram, France) were performed on pure glass and various glass/alumina mixtures (Figure 10).

The dilatometric curve of the glass (Fig. 10.a) shows two characteristic temperatures. The first one is the glass transition temperature T_g (about 815 °C) and the second one is the softening point (about 870 °C). These values confirm that this glass is adapted for a sintering around 850 °C. Various glass/alumina ratios have been tested ranging from 40 to 70 wt% glass [20,21]. The higher the glass concentration is, the larger the shrinkage is important (Figure 10b), that is in agreement with the important shrinkage of the pure glass (i.e. 40%) (Figure 10.a). In order to choose the glass/alumina ratio, the relative density of samples of different glass/alumina ratios sintered at 850 °C for one hour, was measured (Table 1).

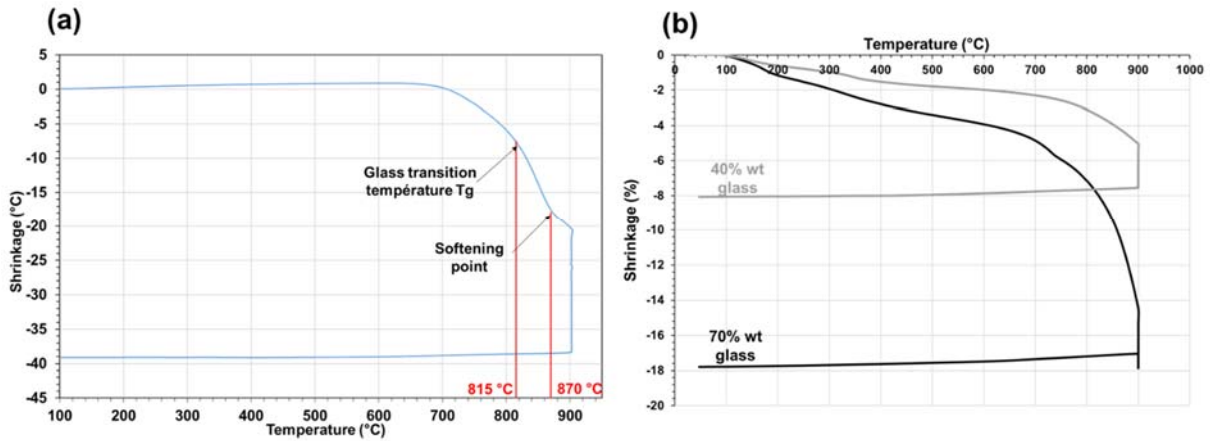


Figure 10: Thermal analysis of the materials used: (a) Dilatometry of glass and (b) dilatometry of alumina/glass system

Table 1 Relative densities of samples of different glass / alumina ratios sintered at 850 °C for one hour

Ratio glass/alumina (m%)	40/60	50/50	60/40	70/30
Relative density (%)	79	93	95	97

In order to control the dimensional resolution of the LTCC components as well as densification close to 100%, the glass/alumina ratio was fixed at 70 wt% glass – 30 wt% alumina which correspond to a classical shrinkage of 18% at the sintering temperature of 850 °C (1 h) recommended by the supplier of the silver paste. This 70/30 wt% glass/alumina ratio is classically found in the literature [5,19,22–24] for LTCC dielectric material. Coefficient of Thermal Expansion (CTE) of the 70 wt% glass/30 wt% alumina, measured by dilatometry, is $5.6 \cdot 10^{-6} \text{ K}^{-1}$ and the thermal conductivity measured by the flash laser technic (LFA427, Netzsch, Germany), is of the order of $1.7 \text{ W} \cdot \text{m}^{-1} \cdot \text{K}^{-1}$.

The stereolithography paste containing 71 wt% mixture powder (glass/alumina) powder and 29 wt% of organics (photoinitiator, monomer/oligomer, binder,...) was formulated by 3DCeram-sinto, Limoges (France). The paste has a shear thinning rheological behavior, necessary for the spreading of thin layers with a viscosity of 26.1 Pa.s at 20 s^{-1} .

A critical step of the process of LTCC components by additive technologies is the debinding and the co-sintering of ceramic/metal parts. The thermal cycle requires to eliminate the organic components without cracking and to obtain a dense part. Both the glass/alumina stereolithography and the silver extrusion pastes were characterized by TGA/DSC

(Thermogravimetric Analysis /Differential Scanning Calorimetry - Labsys-evo-1600, Setaram, France) in order to define the debinding thermal cycle (Figure 11).

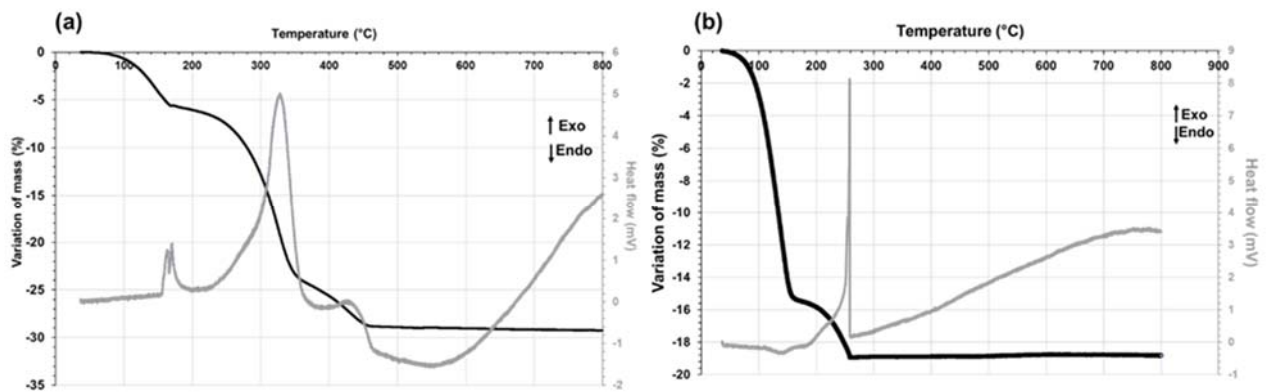


Fig. 11. Thermal analysis under air of (a) LTCC stereolithography glass/alumina system (b) commercial silver paste

The elimination of organic components from the stereolithography paste and from the silver paste is complete around 460 and 250 °C, respectively (Figure 10 and b). To be sure that no more organic remains in a component with a thickness of some mm, a temperature of debinding of 600 °C during 3 hours was retained. In order to avoid phenomena of cracking or bubble formation due to the presence of glass, a slow heating rate lower than 1 °C/min was adopted. The resulting thermal cycle is reported in Figure 12. No weight gain was observed on the TGA of the silver up to 850 °C that suggest that no oxidation of the silver occurs. This point will be further verified by the electrical characterization.

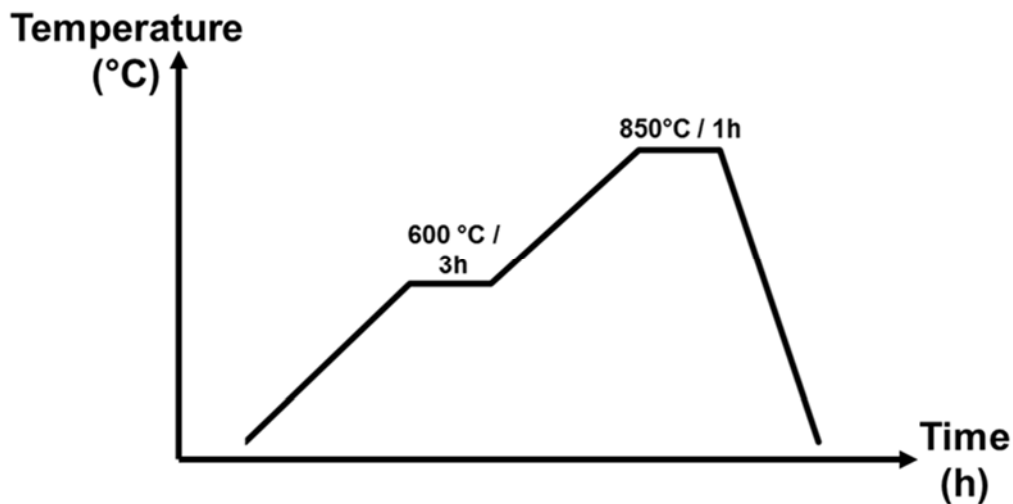


Figure 12: Thermal cycle for debinding and sintering of LTCC parts under air

Printed multi material parts are sintered according to this cycle (Figure 13).

The uncovered tracks (Figure 13.a) have a width of $130\ \mu\text{m}$ and a thickness of $20\ \mu\text{m}$. Vias (Figure 13.b) have a diameter of $250\ \mu\text{m}$ and a depth of $400\ \mu\text{m}$. A circular silver armor was printed around a via (Figure 13.c), in order to improve the performance of current circuits. The diameter of the armor is $4.4\ \text{mm}$, a width of $250\ \mu\text{m}$ and a depth of $400\ \mu\text{m}$. The oblique via (Figure 13.e), makes it possible to avoid several vertical and horizontal transitions to connect two tracks shifted along the x, y and z-axis, has a diameter of $250\ \mu\text{m}$ and a depth of $400\ \mu\text{m}$.

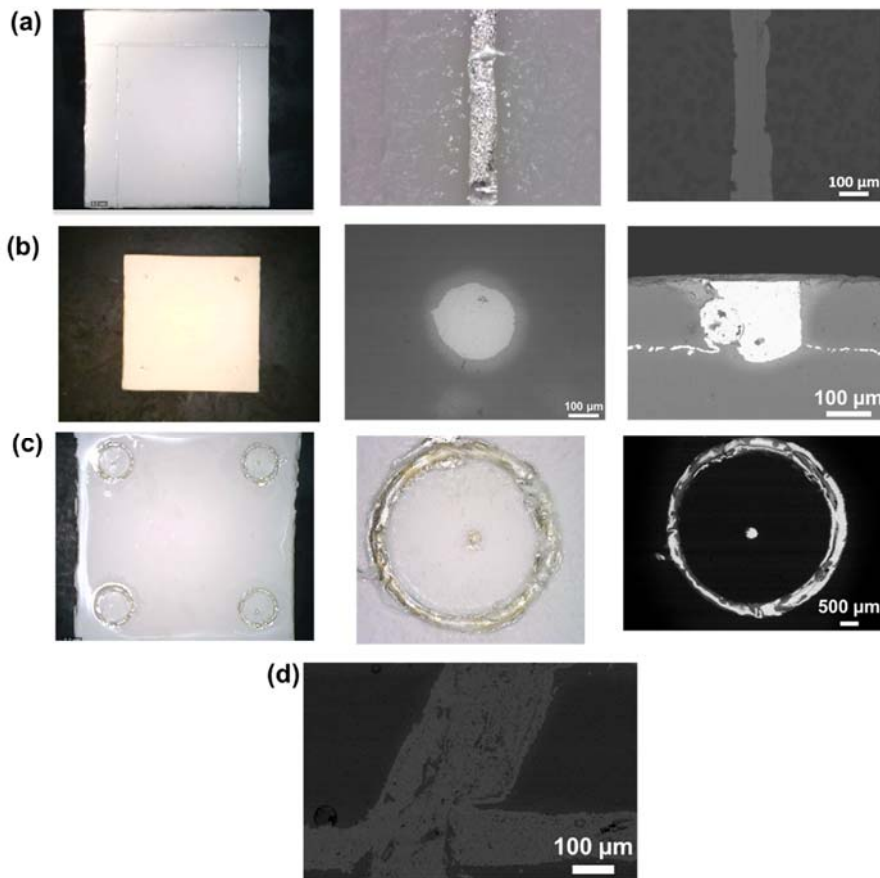


Figure 11: Optical and electronic microscopy of LTCC multi-materials parts: (a) uncovered tracks, (b) embedded track connected to surface by vias, (c) armored vias, and (d) oblique vias after heat treatment at $850\ ^\circ\text{C}/1\ \text{h}$ under air

3.3. Mechanical characterizations

The mechanical characteristics of the substrate, after debinding and sintering, according to the thermal cycle given **Erreur ! Source du renvoi introuvable.**, are measured. The relative density of the LTCC substrate without the silver tracks, measured by the Archimedes' method using ethanol as the inhibiting liquid, is 97%.

The mechanical characteristics are measured using 4-point bending test. The Young's modulus E and the flexural strength σ_f are determined using the classical theory of beams:

$$E = \frac{F_{max} L^3}{8bh^3\Delta y} \quad \text{Eq. 1}$$

$$\sigma_{max} = \frac{3(L-l)F_{max}}{2bh^2} \quad \text{Eq. 2}$$

where Δy is the displacement of the machine, L the distance between bottom supports (40 mm) and l (20 mm) the distance between upper supports, b and h the width and the thickness of the beam respectively, and F the maximal load at rupture. The flexural strength and the Young modulus values given Table 2 are in agreement with the characteristics usually found in the literature for a LTCC dielectric substrate [9,25,26].

Table 2: Mechanical characteristics of the dielectric substrate after sintering at 850 °C for 1h (10 samples)

	σ_f (MPa)	Young modulus (GPa)
850°C / 1h	84 ± 24	83 ± 24

3.4. Electrical characterization

The electrical resistance of the tracks was measured by the 4-points method on the first geometry (Figure 5.a). For more precision of the measurement, a platinum wire was bond with a platinum paste to the places where the measures have to be carried out. The resistivity, ρ_{track} , of the tracks is calculated using:

$$\rho_{track} = \frac{R \times S}{l} \quad \text{Eq. 3}$$

where l and S are the length and the section of the track respectively, and R the measured resistance.

In both cases of uncovered tracks and embedded tracks with vias (Figure 5.c), similar resistivity values of $2.8 \cdot 10^{-8} \Omega \cdot m$ for a line length of 20 mm was measured. The localization of the track inside the dielectric part (embedded) does not induce a decrease in conductivity that suggests that the embedded track is not damaged and the vias are well aligned with the tracks. The Table 3 compares our work with results of the literature obtained with silver tracks but not necessarily using the same substrates or the same processes.

Table 3: Comparison between the resistivity obtained in this study with the literature

Reference	Substrate	Metal	Process	Sintering temperature (°C)	Time (min)	Resistivity (Ω.m)
Present work	Glass/alumina	80% Ag	Robocasting	850	60	$5.5 \cdot 10^{-8}$
Faddoul et al.[8]	LTCC – DP951 (Dupont)	70% Ag – 3 μm	Screen printing	875	60	$3 \cdot 10^{-8}$
Luo et al.[29]	Glass/alumina	Commercial paste TC0307 Ag (Heraeus)	Screen printing	825	30	$4.5 \cdot 10^{-8}$
Lahti et Lantto [28]	Commercial DP943 (Dupont)	D-901-CT (ESL) and HF602 (Dupont tapes) Ag	Gravure-offset printing	850 and 875	/	$5 \cdot 10^{-8}$
Faddoul et al. [27]	Alumina	70% Ag – 3 μm	Flexography	700	15	$6 \cdot 10^{-8}$
Songping [30]	Ferrite	60 – 70% Ag 1-2μm	/	850	15	$15 \cdot 10^{-8}$

The obtained values of resistivity are similar to those reported in the literature, though our hybrid process is very different to the classical ones with the advantage to be able to build more complex geometries and continuous armors.

3.5. Hyper frequency characterizations

The glass/alumina dielectric material has been characterized in the microwave frequencies range. In this respect, the permittivity and the dielectric losses of the substrate have been measured at 12 GHz by the coupled resonator method [31-33]. At this frequency, the permittivity of the substrate is $\epsilon_r = 5.05$ and the loss tangent $\text{tg}\delta = 1.8 \cdot 10^{-3}$ at 20°C. Moreover, the temperature coefficient $\tau\epsilon$, measured between 20 and 80 °C, is $48 \cdot 10^{-6} \text{ K}^{-1}$. The permittivity, the loss tangent and the temperature coefficient of this dielectric substrate corresponds to values found in the literature for LTCC substrates and the losses show that the glass/alumina mixture can be considered as a good material for application in the high frequencies [26,34].

High frequencies characterizations were also performed on micro strip line geometry. A geometry very close to those presented in Figure 6 has been fabricated. The Figure 12 confirms the feasibility of such a geometry using the developed hybrid machine. A line with a width of 600 microns and a space between the line and the ground plane of 300 microns is obtained. These dimensions are very similar to those simulated. In addition, metal walls are obtained from both sides of the line, which is really an advance for this type of circuit. These are connected to a ground plane embedded in the dielectric substrate. The next step is to

characterize these components in microwave frequencies. Subsequently, it will be necessary to improve the filling of the ground plane and the position of the studied strip.

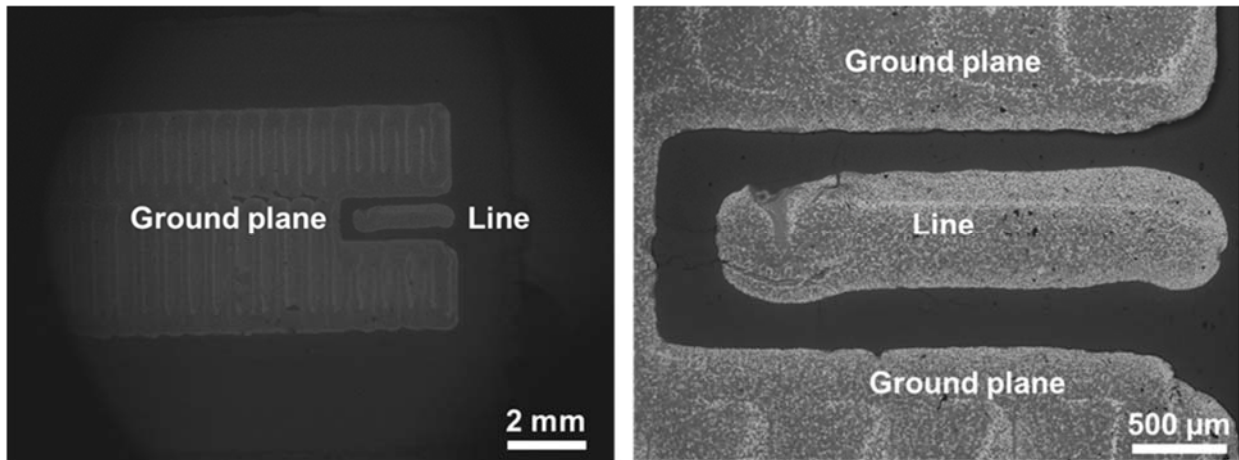


Figure 12 : Micrograph of an embedded micro strip resonator in LTCC materials

4. Conclusion

A new hybrid machine has been designed to obtain monolithic multi-material parts, consisting in the association of a stereolithography machine and a robotic arm able to control a robocasting head. This hybrid machine makes it possible to build parts consisting in a dielectric substrate, realized using a stereolithography process and metal tracks deposited by robocasting. LTCC components fabricated using this hybrid machine are sintered under air at 850 °C for 1 h. The dense final parts have mechanical properties close to those obtained by conventional methods with a Young modulus $E=83 \pm 24$ GPa and a flexural strength $\sigma_f=84 \pm 24$ MPa. The metal tracks have a minimum width of 110 microns and a maximum thickness of 20 microns after sintering. Their resistivity is near $2.8 \cdot 10^{-8} \Omega \cdot m$, which is close to the best results found in the literature. The presented printed parts have more or less complex geometries, ranging from an uncoated track to micro strip line.

These results demonstrate the feasibility, by a flexible additive manufacturing process, of complex 3D metallic networks in a dielectric material, which is attractive for LTCC, HTCC or other electronic components. For instance, metallic armors and oblique vias can be elaborated using this hybrid process, which is not possible using conventional routes (i.e. tape casting and screen-printing). To extend the applications, HTCC components also used in microelectronics will be built.

References

- [1] C. Robert, *Fiabilité des assemblages de puissance*, Thèse de l'Université de Paris-Saclay, 2015.
- [2] W. Bakalski, et al., 5-6.5 GHz LTCC power amplifier module with 0.3 W at 2.4 V in Si-bipolar, *Electron. Lett.* 39 (February (4)) (2003).
- [3] C.Q. Scrantom, J.C. Lawson, LTCC technology: where we are and where we're going. II, 1999 IEEE MTT-S International Topical Symposium on Technologies for Wireless Applications (Cat. No. 99TH8390) (1999) 193–200.
- [4] H.D. Smith, D.F. Elwell, HTCC/LTCC use of multiple ceramic tapes in high rate production, US5318820A, 07-Jun-1994.
- [5] I.J. Induja, K.P. Surendran, M.R. Varma, M.T. Sebastian, Low κ , low loss aluminaglass composite with low CTE for LTCC microelectronic applications, *Ceram. Int.* 43 (January (1) Part A) (2017) 736–740.
- [6] R. Faddoul, *Optimisation des procédés d'impression dédiés à la production de masse de composants microélectroniques*, Université Grenoble Alpes, 2012 Thèse de doctorat.
- [7] R. Faddoul, N. Reverdy-Bruas, A. Blayo, B. Khelifi, Inkjet printing of silver nanosuspensions on ceramic substrates – sintering temperature effect on electrical properties, *Microelectron. Eng.* 105 (May) (2013) 31–39.
- [8] R. Faddoul, N. Reverdy-Bruas, A. Blayo, Formulation and screen printing of water based conductive flake silver pastes onto green ceramic tapes for electronic applications, *Mater. Sci. Eng. B* 177 (August (13)) (2012) 1053–1066.
- [9] A. Khalil, *Technologies LTCC et stéréolithographie céramique 3D appliquées à la conception de dispositifs millimétriques et sub-millimétriques*, (2010).
- [10] L. Ren, X. Luo, H. Zhou, The tape casting process for manufacturing lowtemperature co-fired ceramic green sheets: a review, *J. Am. Ceram. Soc.* 101 (September (9)) (2018) 3874–3889.
- [11] C. Dupas, *Elaboration par stéréolithographie de métamatériaux tout diélectrique pour le domaine du térahertz*, Université de Limoges, 2016 Thèse de doctorat.
- [12] P.F. Jacobs, *Rapid Prototyping & Manufacturing: Fundamentals of Stereolithography*, Society of Manufacturing Engineers, 1992.
- [13] T. Chartier, et al., Additive manufacturing to produce complex 3D ceramic parts, *J. Ceram. Sci. Technol.* 6 (2) (2015) 95–104.
- [14] R.N. Leyden, T.A. Almouist, M.A. Lewis, H.D. Nguyen, Stereolithography method and apparatus, US5143663A, 01-Sep-1992.
- [15] T. Maeder, *Assemblage de matériaux céramiques*, (2004).
- [16] H. Zhu, M. Liu, H. Zhou, L. Li, A. Lv, Preparation and properties of low-temperature co-fired ceramic of CaO–SiO₂–B₂O₃ system, *J. Mater. Sci.: Mater. Electron.* 17 (August (8)) (2006) 637–641.
- [17] M. Sebastian, R. Uvic, H. Jantunen, Low-loss dielectric ceramic materials and their properties, *Int. Mater. Rev.* 60 (July) (2015) 1743280415Y.000.
- [18] A. Baker, et al., Integration concepts for the fabrication of LTCC structures, *Int. J. Appl. Ceram. Technol.* 2 (November (6)) (2005) 514–520.
- [19] Q. Wu, S. Hu, Y. Chai, *Preparation and Characterization of Printed LTCC Substrates for Microwave Devices*, (2014).
- [20] X. Luo, et al., Microstructure, sintering and properties of CaO–Al₂O₃–B₂O₃–SiO₂ glass/Al₂O₃ composites with different CaO contents, *J. Mater. Sci.: Mater. Electron.* 27 (May (5)) (2016) 5446–5451.
- [21] I.J. Induja, P. Abhilash, S. Arun, K.P. Surendran, M.T. Sebastian, LTCC tapes based on Al₂O₃–BBSZ glass with improved thermal conductivity, *Ceram. Int.* 41 (December (10), Part A) (2015) 13572–13581.
- [22] H.-I. Hsiang, L.-T. Mei, S.-W. Yang, W.-C. Liao, F.-S. Yen, Effects of alumina on the crystallization behavior, densification and dielectric properties of BaO–ZnO–SrO–CaO–Nd₂O₃–TiO₂–B₂O₃–SiO₂ glass–ceramics, *Ceram. Int.* 37 (September (7)) (2011) 2453–2458.

- [23] Y.J. Seo, D.J. Shin, Y.S. Cho, Phase evolution and microwave dielectric properties of lanthanum borate-based low-temperature co-fired ceramics materials, *J. Am. Ceram. Soc.* 89 (7) (2006) 2352–2355.
- [24] K.M. Nowak, H.J. Baker, D.R. Hall, Cold processing of green state LTCC with a CO₂ laser, *Appl. Phys. A* 84 (August (3)) (2006) 267–270.
- [25] L. Golonka, Technology and applications of low temperature co-fired ceramic (LTCC) based sensors and microsystems, *Bull. Polish Acad. Sci. Tech. Sci.* 54 (June) (2006).
- [26] H. Jantunen, T. Kangasvieri, J. Vähäkangas, S. Leppävuori, Design aspects of microwave components with LTCC technique, *J. Eur. Ceram. Soc.* 23 (January (14)) (2003) 2541–2548.
- [27] R. Faddoul, N. Reverdy-Bruas, A. Blayo, B. Khelifi, Ink optimization for an alternative way to print on ceramic substrates, Presented at the Proceedings of the 8th International Conference on Multi-Material Micro Manufacture (2011).
- [28] M. Lahti, A. Vimpari, K. Kautio, Printable resistors in LTCC systems, *J. Eur. Ceram. Soc.* 27 (8–9) (2007) 2953–2956.
- [29] J. Luo, R. Eitel, Sintering behavior and biocompatibility of a low temperature cofired ceramic for microfluidic biosensors, *Int. J. Appl. Ceram. Technol.* 14 (March (2)) (2017) 99–107.
- [30] W. Songping, Preparation of micron size flake silver powders for conductive thick films, *J. Mater. Sci.: Mater. Electron.* 18 (April (4)) (2007) 447–452.
- [31] J. Garreau, Étude de filtres hyperfréquence SIW et hybride-planaire SIW en technologie LTCC, Thèse de l'Université de Brest, 2012.
- [32] B. Bianco, M. Parodi, S. Ridella, F. Selvaggi, Launcher and microstrip characterization, *IEEE Trans. Instrum. Meas.* (December) (1976).
- [33] J. Sheen, Amendment of cavity perturbation technique for loss tangent measurement at microwave frequencies, *J. Appl. Phys.* (July) (2007).
- [34] A. Bittner, H. Seidel, U. Schmid, High-frequency characterization of porous low temperature cofired ceramics substrates, *J. Am. Ceram. Soc.* 93 (11) (2010) 3778–3781.